Cancer Chemother Pharmacol (2010) 65:419–425
DOI 10.1007/s00280-009-1044-3

ORIGINAL ARTICLE

Plasma and cerebrospinal fluid pharmacokinetics of ABT-888 after oral administration in non-human primates

Jodi A. Muscal · Patrick A. Thompson · Vincent L. Giranda · Brian D. Dayton · Joy Bauch · Terzah Horton · Leticia McGuffey · Jed G. Nuchtern · Robert C. Dauser · Brian W. Gibson · Susan M. Blaney · Jack M. Su

Received: 14 January 2009 / Accepted: 26 May 2009 / Published online: 13 June 2009

Abstract
Purpose ABT-888 inhibits poly(ADP-ribose) polymerase (PARP) and may enhance the efficacy of chemotherapy and radiation in CNS tumors. We studied the plasma and cerebrospinal fluid (CSF) pharmacokinetics (PK) of ABT-888 in a non-human primate (NHP) model that is highly predictive of human CSF penetration.
Methods ABT-888, 5 mg/kg, was administered orally to three NHPs. Serial blood and CSF samples were obtained. Plasma and CSF concentrations of ABT-888 were measured using LC/MS/MS, and the resulting concentration versus time data were evaluated using non-compartmental and compartmental PK methods.
Results The CSF penetration of ABT-888 was 57 ± 7% (mean ± SD). The peak ABT-888 concentration in the plasma was 0.62 ± 0.18 μM. Plasma and CSF $AUC_{0-\infty}$ were 3.7 ± 1.7 and 2.1 ± 0.8 μM h. PARP inhibition in peripheral blood mononuclear cells was evident 2 h after ABT-888 administration.
Conclusion The CSF penetration of ABT-888 after oral administration was 57%. Plasma and CSF concentrations were in the range that has been shown to inhibit PARP activity in vivo in humans.

Keywords ABT-888 · PARP inhibition · DNA repair · CSF penetration · Pharmacokinetics

Introduction

Poly(ADP-ribose) polymerase (PARP) is a family of enzymes that cleaves nicotinamide adenine dinucleotide (NAD) to nicotinamide and ADP-ribose. The polymerase adds long and branched ADP-ribose polymers onto acceptor proteins, including p53, histones, and DNA repair proteins [27]. This process, termed poly(ADP-ribosyl)ation, leads to unwinding and repair of damaged DNA. PARP-1 binds to single-stranded DNA breaks induced by alkylating agents and to double-stranded breaks formed by ionizing radiation [4, 25]. PARP-2 interacts with PARP-1 and shares common partner proteins [26]. Both PARP enzymes bind to DNA nicks, rapidly halt transcription, and recruit and activate DNA repair proteins involved in base excision repair, non-homologous end joining, and homologous recombination repair pathways [7, 14, 23, 24, 27]. Although there are currently 19 identified members of the PARP family, inhibition of both PARP-1 and -2 is sufficient to stall DNA repair [3, 26].

While PARP activity is critical for repairing DNA damage and maintaining genomic stability in normal cells, tumor cells may use this mechanism to repair DNA damage from chemotherapy and radiation and to avoid apoptosis

This manuscript was presented at the 13th Annual International Symposium on Pediatric Neuro-Oncology, July 2, 2008, Chicago, IL.

J. A. Muscal · P. A. Thompson · T. Horton · L. McGuffey · S. M. Blaney · J. M. Su (✉)
Texas Children's Cancer Center, Baylor College of Medicine, 6621 Fannin Street, MC3-3320, Houston, TX 77030, USA
e-mail: jmsu@txccc.org

V. L. Giranda · B. D. Dayton · J. Bauch
Abbott Laboratories, Abbott Park, IL, USA

J. G. Nuchtern · R. C. Dauser
Texas Childrens's Hospital, Baylor College of Medicine, Houston, TX, USA

B. W. Gibson
Center for Comparative Medicine, Baylor College of Medicine, Houston, TX 77030, USA

[20, 23, 29]. When compared with normal cells, increased PARP expression and activity has been observed in various malignancies [2, 5, 13, 15, 28, 31–33], including gliomas [32] and medulloblastoma (unpublished data).

ABT-888 (Fig. 1) is an orally bioavailable PARP-1 and -2 inhibitor effective at nanomolar concentrations and has been shown to potentiate DNA damaging chemotherapy and radiation [1, 12, 30]. Since PARP overexpression in central nervous system (CNS) tumors may mediate tumor resistance to chemotherapy and radiation, we studied the plasma and cerebrospinal fluid (CSF) pharmacokinetics (PK) of ABT-888 in a non-human primate (NHP) model that is highly predictive of CSF penetration of anti-cancer drugs in humans [18].

Materials and methods

Drug

ABT-888 was supplied by Abbott Laboratories (Abbott Park, IL) in 500 mg vials. The drug was diluted into 20 ml vehicle solution (2.1 g sorbitol, 0.1 g citric acid, monohydrate, and purified water) to a final concentration of 5 mg/ml and administered orally.

Animals

Three adult male rhesus monkeys (*Maccaca mulatta*) weighing 12.5–15 kg were fed Lab Diet 5045 twice daily and were group housed in accordance with the Guide for the Care and Use of Laboratory Animals [21] at Baylor College of Medicine using a protocol approved by the Institutional Animal Care and Use Committee. Blood samples were obtained though a central venous catheter. CSF samples were obtained from a chronically indwelling subcutaneously placed Ommaya reservoir attached to a Pudenz catheter with its tip in the fourth ventricle [18]. The reservoir was pumped several times before each CSF sample collection to ensure adequate mixing with ventricular CSF.

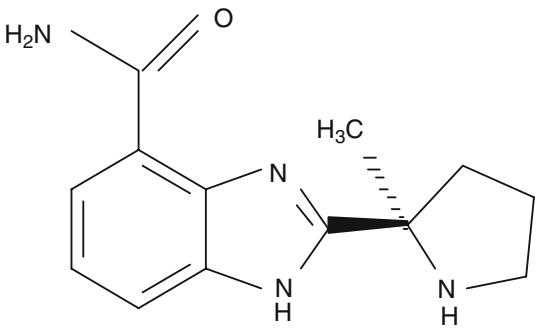

Fig. 1 Chemical structure of ABT-888 (molecular weight 244.29 g/mol)

Experiments

A single 5 mg/kg dose of ABT-888 was administered orally to two NHPs and serial blood samples were obtained at 15, 30, 60, 90 min and 2, 4, 6, 8, and 24 h. These time points were not adequate for determining the terminal half-life, so approximately 6 months later, each animal received another oral dose of ABT-888 and additional sampling points at 3 and 10 h were added. A third animal was also studied using the revised sampling schema. Since the first animal experienced nausea 20 min after ABT-888 administration, subsequent animals received ondansetron (4 mg IV) prior to and 8 h after ABT-888 administration. Serial blood (3 ml) and CSF (0.3 ml) samples were obtained prior to, at 60 and 90 min, and 2, 3, 4, 6, 8, 10, and 12 h after drug administration. Plasma was immediately separated from blood by centrifugation at 4,400 rpm for 10 min at 5°C. Plasma and CSF samples were stored at −80°C until analysis. Clinical laboratory studies including complete blood counts, electrolytes, liver function tests, and renal function tests were obtained at 24 h and weekly for 4 weeks after each ABT-888 administration. Following ABT-888 administration, animals were monitored daily for evidence of toxicity including exams at 24 h and weekly for four consecutive weeks.

Sample analysis

ABT-888 concentrations

Stock solutions of ABT-888 and an internal standard (Abbott proprietary compound A-092274, concentration 0.55 mcg/ml) were prepared by dissolving each in a mixture of DMSO and 0.1% trifluoroacetic acid. Serial dilutions were prepared in either heparinized monkey plasma (Lampire Biological Laboratories, Pipersville, PA) or CNS perfusion fluid (CMA Microdialysis, Chelmsford, PA). To all plasma samples and standards, 0.2 ml of 0.5 M Na_2CO_3 was added, followed by 0.9 ml of a 1:1 mixture of ethyl acetate:hexane. Samples were vortexed for 30 s and centrifuged at 3,000 rpm to separate phases. The organic layer was removed, evaporated to dryness under nitrogen, and then reconstituted in 0.3 ml of acetonitrile:1% (v/v) formic acid (5:95, v/v). For the CSF samples and standards, 0.02 ml of acetonitrile containing 10% (v/v) DMSO was added. The samples were vortexed and then 20 µL of sample was injected for analysis.

ABT-888 and the internal standard were separated from each other and coextracted contaminants on a 50 × 3 mm Keystone Aquasil 5 µm C18 column with an

acetonitrile:1% formic acid mobile phase (11:89 by volume) at a flow rate of 0.4 ml/min. Analysis was done on a Sciex API3000 Biomolecular Mass Analyzer with a turboionspray interface using Sciex TurboQuan^{TM} software. The lower limits of detection for ABT-888 were 4 ng/ml (16 nM) for CSF samples and 6 ng/ml (24 nM) for plasma samples. Range of linearity for both the plasma and CSF assay was 4 ng/ml–5 μg/ml (0.016–20.5 μM). Each concentration was determined in triplicate. For the plasma samples, the coefficient of variation (CV) was 1–16% for concentrations below 0.4 μM and 6–10% above 0.4 μM. For the CSF samples, the CV was 6–28% for concentrations below 0.4 μM and 8–12% above 0.4 μM.

PARP activity in peripheral blood mononuclear cells

Heparinized peripheral blood (1–1.5 ml) was obtained from three animals, and peripheral blood mononuclear cells (PBMCs) were isolated using Lymphoprep solution (Axis-Shield, Oslo, Norway). PBMCs were obtained before ABT-888 treatment and at 2 h after ABT-888 administration. Proteins lysates were prepared according to the manufacturer's directions (HT chemiluminescent PARP/Apoptosis Assay; Trevigen, Gaithersburg, MD). PARP bioluminescent activity was measured using a Luminoscan Ascent luminometer (ThermoFisher Scientific, Waltham, MA). The measurements were performed in triplicate and repeated in two independent experiments.

Pharmacokinetic analysis

Non-compartmental methods were used to calculate the area under the concentration–time curve (AUC), apparent total body clearance (Cl_{TB}/F), and apparent steady-state volume of distribution (Vd_{ss}/F). The $AUC_{0-\infty}$ was estimated using the linear trapezoidal method to the last time point and then extrapolation to infinity based on the last measured concentration and the terminal rate constant. Cl_{TB}/F was derived by dividing the dose by the $AUC_{0-\infty}$. Vd_{ss}/F was calculated using the area under the moment curve (AUMC) [22]. CSF penetration of ABT-888 was calculated as $AUC^{CSF}_{0-\infty}/AUC^{plasma}_{0-\infty}$. The half-life ($t_{1/2}$) was estimated assuming first-order kinetics. Volume of distribution and clearance are reported as apparent parameters (Vd_{ss}/F and Cl_{TB}/F where F represents bioavailability). This nomenclature is commonly used in studies of oral drugs in which bioavailability is not known or measured.

Additionally, a PK model that could be simultaneously fit to the plasma and CSF concentration–time data for each animal was developed using ADAPT II software [10]. Figure 2 shows a schematic of the compartmental model, which included the following: (1) a time delay for absorption, (2) first-order absorption kinetics, (3) first-order elimination, (4) equilibrium between the CSF and plasma, and (5) a CSF volume fixed to 10 ml [27, 28].

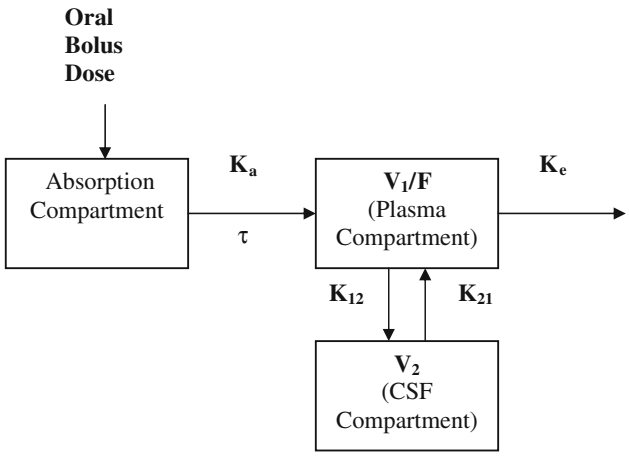

Fig. 2 Schematic of the PK model for ABT-888 in non-human primates. The PK model for describing the plasma and CSF disposition of ABT-888 consists of an absorption compartment, a plasma compartment, and a CSF compartment. The model uses first-order absorption with a variable minute lag time, linear irreversible elimination from the plasma compartment, and linear transfer between plasma and CSF

Results

Pharmacokinetics parameters after a single 5 mg/kg oral dose of ABT-888 are presented in Table 1. Peak ABT-888 concentrations in the plasma (C^{P}_{max}) were 0.62 ± 0.18 μM (mean ± SD). Plasma $AUC_{0-\infty}$ was 3.7 ± 1.7 μM h and the fraction of the AUC that was extrapolated to infinity from the final time point varied from 12 to 21%. The plasma $t_{1/2}$ was 3.4 ± 0.6 h. The Cl_{TB}/F was 6.3 ± 2.4 L/h/kg, and the Vd_{ss}/F was 38 ± 8 L/kg. The CSF C_{max}, which was observed between 3 and 6 h after ABT-888 administration, was 0.23 ± 0.12 μM. The CSF $AUC_{0-\infty}$ was 2.1 ± 0.8 μM h and the fraction of the AUC that was extrapolated to infinity from the final time point varied from 16 to 40%. The CSF penetration of ABT-888 was 57 ± 7%.

The model parameters are shown in Table 2. Disappearance from the plasma was best described by first-order kinetics. Absorption kinetics were difficult to characterize because the sampling algorithm was designed to characterize exposure and clearance, and the time delay for absorption was variable (range 46–165 min). K_{12} and K_{21} were estimated by fitting the model to the plasma and CSF concentration versus time data. The clearance from the CSF was estimated to be 7.1 ± 2.6 ml/h. Comparisons of the measured and modeled plasma and CSF concentration versus time profiles for the three animals are shown in

Table 1 Non-compartmental plasma and CSF PK parameters of ABT-888 after a single oral 5 mg/kg dose in non-human primates

Animal	C^{P}_{max} (μM)	$AUC^{P}_{0-\infty}$ (μM h)	Cl_{TB}/F (L/h/kg)	Vd_{ss}/F (L/kg)	$t^{P}_{1/2}$ (h)	C^{CSF}_{max} (μM)	$AUC^{CSF}_{0-\infty}$ (μM h)	CSF penetration (%)
1	0.45	2.4	8.5	46	3.7	0.15	1.4	56
2	0.60	3.0	6.7	38	3.1	0.16	2.0	64
3	0.81	5.6	3.7	29	3.4	0.37	2.8	51
Mean	0.62	3.7	6.3	38	3.4	0.23	2.1	57
SD	0.18	1.7	2.4	8	0.6	0.12	0.8	7

All parameters reported to two significant digits

C^{P}_{max} maximum plasma concentration, $AUC^{P}_{0-\infty}$ area under the curve extrapolated to infinity, Cl_{TB}/F apparent clearance, Vd_{ss}/F apparent volume of distribution, $t^{P}_{1/2}$ plasma half-life, C^{CSF}_{max} maximum CSF concentration, $AUC^{CSF}_{0-\infty}$ area under the curve extrapolated to infinity, *CSF penetration* $AUC^{CSF}_{0-\infty}/AUC^{P}_{0-\infty} \times 100$

Table 2 Simultaneous plasma and CSF PK parameters after a single 5 mg/kg dose in non-human primates

Animal	τ (h)	K_a (h^{-1})	V_1/F (L/kg)	K_e (h^{-1})	K_{12} (h^{-1})	K_{21} (h^{-1})	$t^{P}_{1/2}$ (h)	CSF CL (ml/h)
1	0.76	12.5	41.5	0.23	7.0×10^{-6}	0.805	3.0	8.1
2	0.78	53.5	40.0	0.18	4.7×10^{-6}	0.420	3.9	4.2
3	2.75	44.2	24.2	0.16	16.5×10^{-6}	0.913	4.3	9.1
Mean	1.43	36.7	35.2	0.19	9.4×10^{-6}	0.71	3.7	7.1
SD	1.14	21.5	9.6	0.04	6.3×10^{-6}	0.26	0.7	2.6

τ time-delay for absorption of oral drug, K_a absorption rate constant, V_1/F model-estimated apparent volume of distribution, K_e plasma elimination rate constant, K_{12} rate constant for transfer from plasma to CSF, K_{21} rate constant for transfer from CSF to plasma, $t^{P}_{1/2}$ model-estimated plasma half-life, *CSF CL* clearance from CSF

Fig. 3a–c. As the figures show, model fits for each animal were very good. The R^2 values for the plasma concentration–time fits ranged from 0.91 to 0.99 and the R^2 for the CSF concentration–time fits were 0.95–0.99.

Compared with pre-treatment levels, at 2 h after a single dose of ABT-888, PARP activity in PBMCs from all three animals was drastically reduced (67 ± 13%) (Table 3). Similar to the variable baseline PARP activity that has been reported in humans (S. Kummar, personal communication), animal 3 had a much higher pre-treatment PARP level (2.02 units/mg protein) compared with the other two animals (0.25 and 0.24 units/mg protein, respectively) but similarly showed a dramatic reduction in PARP activity post-treatment.

All animals tolerated ABT-888 quite well. With the exception of a single episode of emesis that occurred in the first animal, there was no other observed clinical toxicity. In addition, no abnormalities in laboratory parameters were noted in the 4 weeks after ABT-888 dosing.

Discussion

Poly(ADP-ribose) polymerase is a critical enzyme for activating multiple DNA repair pathways following DNA damage. Because PARP is over-expressed in various human tumors, including CNS tumors [32], increases in PARP activity and enhanced DNA repair may mediate tumor resistance to chemotherapy and radiation. Pre-clinical studies have confirmed that PARP inhibition enhances cytotoxicity to many chemotherapy agents, including temozolomide [8, 9, 30], topoisomerase I inhibitors irinotecan and topotecan [6, 11], and platin compounds [19]. In addition, PARP inhibition potentiates the anti-tumor effect of chemotherapy for intracranial xenografts, including CNS tumors [8, 9, 30].

ABT-888 is an orally bioavailable, potent PARP inhibitor with $K_i s$ of 3.6 and 2.9 nM for PARP-1 and -2 inhibition, respectively [12]. Protein binding values in plasma (assessed in vitro as % bound at 5 μM) for ABT-888 were moderate in all species, averaging 42% in dog, 41% in monkey, 43% in mouse, 49% in rat and 51% in human. In vivo studies demonstrate that ABT-888 potentiates the anti-tumor activity of temozolomide, cisplatin, carboplatin, and cyclophosphamide against various human cancer xenografts [12]. Recent studies also show that ABT-888 potentiates radiation against human colon cancer [12] and lung cancer xenograft models [1].

Since ABT-888 enhances chemotherapy and radiation and has been shown in CD-1 mice to preferentially accumulate in intracranial tumors versus normal brain [12], we studied the plasma and CSF PK of ABT-888 in a NHP model that previously has been shown to be predictive of CSF drug penetration in humans [18]. We demonstrated

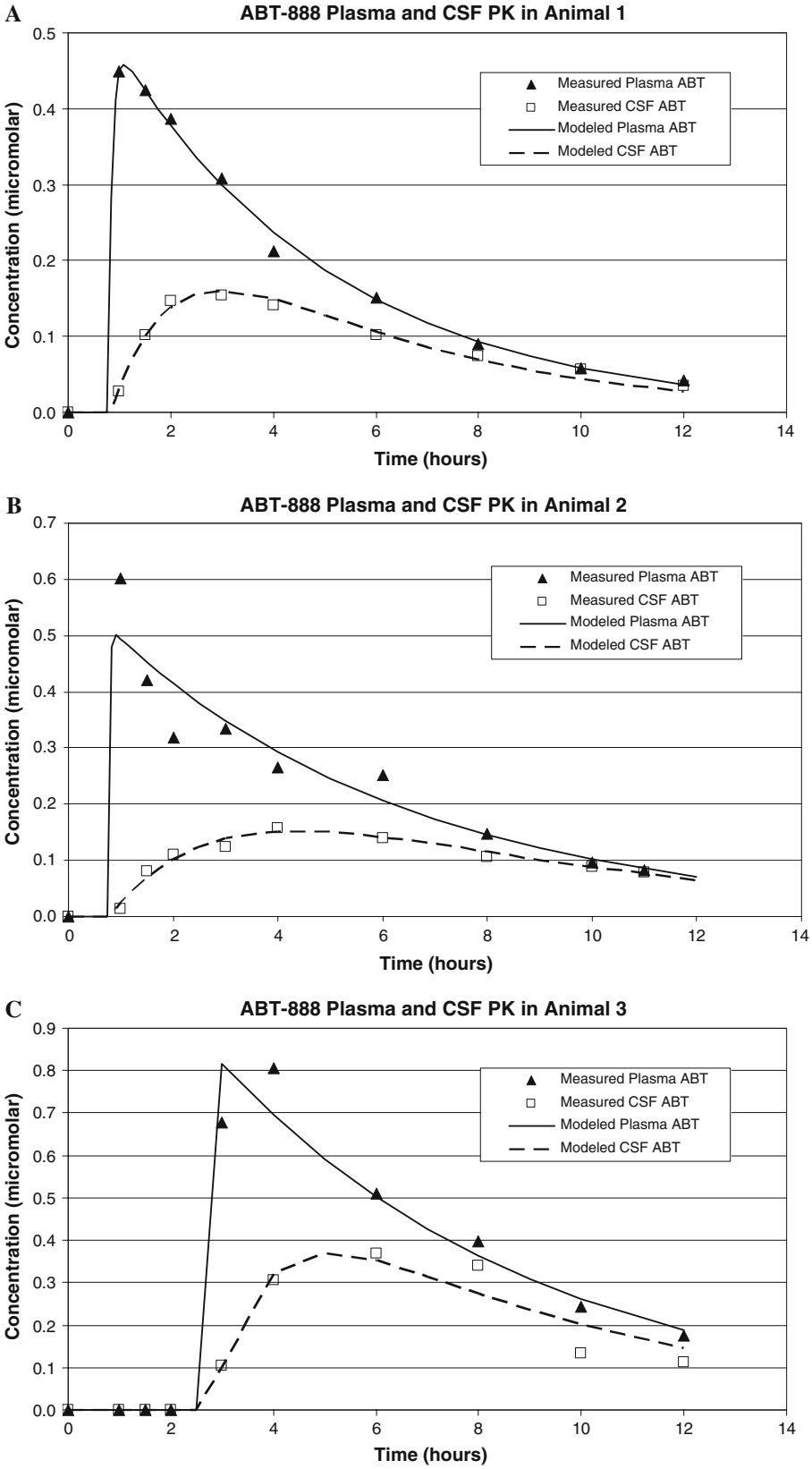

Fig. 3 Model predicted versus measured ABT-888 concentrations in plasma and CSF for three non-human primates. The *lines* represent the model predictions and the *symbols* the data points. The *solid lines* represent the plasma ABT-888 model estimates and the *dashed lines* the CSF ABT-888 estimates. The *triangles* represent the measured plasma ABT-888 and the *open squares* the CSF ABT-888

Table 3 Inhibition of PARP activity in peripheral blood mononuclear cells

Serum PARP activity and % PARP inhibition			
Animal	PARP activity (units/mg protein) ± SD		
	Pre-treatment	2 h post-ABT-888	% PARP inhibition
1	0.25 ± 0.01	0.12 ± 0.01	52
2	0.24 ± 0.01	0.07 ± 0.02	71
3	2.02 ± 0.08	0.44 ± 0.02	78

% PARP inhibition = 100 × [(pre-treatment) − (2 h post)]/(pre-treatment)

that there was substantial ABT-888 present in the CSF following oral dosing. The serum and CSF ABT-888 exposures in our model approached or exceeded those exposures required for PARP inhibition in preclinical and phase 0 studies [16, 17]. For example, the mean CSF C_{max} in our NHP model (0.23 ± 0.12 μM after a single 5 mg/kg oral dose of ABT-888) was comparable to the concentrations (0.1–0.3 μM) required for ex vivo PARP inhibition in PBMCs [17]. Thus, ABT-888 may enhance the cytotoxicity of agents known to penetrate the blood–brain barrier, such as temozolomide and topotecan, and have the potential to minimize leptomeningeal dissemination of malignancies with a known predilection for such spread.

In a phase 0 study of ABT-888 at the National Cancer Institute, >90% PARP inhibition was observed in PBMCs and biopsied tumors after a single oral dose of 25 or 50 mg of ABT-888 [16, 17]. We also evaluated the extent of PARP inhibition in the NHP PBMCs following a single oral dose of ABT-888 (5 mg/kg, equivalent to ~55 mg in human) and observed that there was a similar degree of PARP inhibition (range 52–78%) 2 h after ABT-888 administration. Investigation of ABT-888 has moved into phase I trials in solid tumors in adults in combination with (1) temozolomide, (2) cyclophosphamide, (3) carboplatin and paclitaxel, or (4) topotecan (http://www.clinicaltrials.gov). In our NHP model, the observed mean plasma C_{max} (0.62 ± 0.18 μM) is comparable to C_{max} observed after multiple oral dosing in clinical trials (V. Giranda, personal communication).

In summary, ABT-888 is a potent inhibitor of PARP-1 and -2 that potentiates chemotherapy and radiation against CNS tumors in animal studies. PK data from our NHP model shows that, as in rodents, there is substantial CSF exposure after oral dosing. Our data suggest that ABT-888 concentrations in plasma and CSF are sufficient to adequately inhibit PARP activity of primary or metastatic CNS or leptomeningeal tumors and therefore may potentiate anti-tumor effect of chemotherapy and/or radiation. Early phase clinical trials to evaluate ABT-888 in combination with radiation and/or chemotherapy in CNS tumors are currently in development.

Acknowledgments We thank Gaye Jenkins for technical assistance. National Cancer Institute K12 Pediatric Clinical Oncology Research Training Program 5K12CA90433-07 (JA Muscal), Mentored Specialized Clinical Investigator Development Award in Pediatric Pharmacology (PA Thompson), The Childhood Brain Tumor Foundation (JM Su), National Cancer Institute K23 Career Development Award 1K23CA113721 (JM Su).

References

1. Albert JM, Cao C, Kim KW, Willey CD, Geng L, Xiao D, Wang H, Sandler A, Johnson DH, Colevas AD, Low J, Rothenberg ML, Lu B (2007) Inhibition of poly(ADP-ribose) polymerase enhances cell death and improves tumor growth delay in irradiated lung cancer models. Clin Cancer Res 13:3033–3042
2. Alderson T (1990) New targets for cancer chemotherapy—poly(ADP-ribosylation) processing and polyisoprene metabolism. Biol Rev Camb Philos Soc 65:623–641
3. Ame JC, Rolli V, Schreiber V, Niedergang C, Apiou F, Decker P, Muller S, Hoger T, Menissier-de Murcia J, de Murcia G (1999) PARP-2, A novel mammalian DNA damage-dependent poly(-ADP-ribose) polymerase. J Biol Chem 274:17860–17868
4. Ame JC, Spenlehauer C, de Murcia G (2004) The PARP superfamily. Bioessays 26:882–893
5. Berger NA, Adams JW, Sikorski GW, Petzold SJ, Shearer WT (1978) Synthesis of DNA and poly(adenosine diphosphate ribose) in normal and chronic lymphocytic leukemia lymphocytes. J Clin Invest 62:111–118
6. Bowman KJ, Newell DR, Calvert AH, Curtin NJ (2001) Differential effects of the poly (ADP-ribose) polymerase (PARP) inhibitor NU1025 on topoisomerase I and II inhibitor cytotoxicity in L1210 cells in vitro. Br J Cancer 84:106–112
7. Bryant HE, Helleday T (2006) Inhibition of poly (ADP-ribose) polymerase activates ATM which is required for subsequent homologous recombination repair. Nucleic Acids Res 34:1685–1691
8. Calabrese CR, Almassy R, Barton S, Batey MA, Calvert AH, Canan-Koch S, Durkacz BW, Hostomsky Z, Kumpf RA, Kyle S, Li J, Maegley K, Newell DR, Notarianni E, Stratford IJ, Skalitzky D, Thomas HD, Wang LZ, Webber SE, Williams KJ, Curtin NJ (2004) Anticancer chemosensitization and radiosensitization by the novel poly(ADP-ribose) polymerase-1 inhibitor AG14361. J Natl Cancer Inst 96:56–67
9. Cheng CL, Johnson SP, Keir ST, Quinn JA, Ali-Osman F, Szabo C, Li H, Salzman AL, Dolan ME, Modrich P, Bigner DD, Friedman HS (2005) Poly(ADP-ribose) polymerase-1 inhibition reverses temozolomide resistance in a DNA mismatch repair-deficient malignant glioma xenograft. Mol Cancer Ther 4:1364–1368
10. D'Argenio D (1997) ADAPT II user's guide: pharmacokinetic/pharmacodynamic systems analysis software. University of Southern California, Los Angeles
11. Delaney CA, Wang LZ, Kyle S, White AW, Calvert AH, Curtin NJ, Durkacz BW, Hostomsky Z, Newell DR (2000) Potentiation of temozolomide and topotecan growth inhibition and cytotoxicity by novel poly(adenosine diphosphoribose) polymerase inhibitors in a panel of human tumor cell lines. Clin Cancer Res 6:2860–2867
12. Donawho CK, Luo Y, Luo Y, Penning TD, Bauch JL, Bouska JJ, Bontcheva-Diaz VD, Cox BF, DeWeese TL, Dillehay LE,

Ferguson DC, Ghoreishi-Haack NS, Grimm DR, Guan R, Han EK, Holley-Shanks RR, Hristov B, Idler KB, Jarvis K, Johnson EF, Kleinberg LR, Klinghofer V, Lasko LM, Liu X, Marsh KC, McGonigal TP, Meulbroek JA, Olson AM, Palma JP, Rodriguez LE, Shi Y, Stavropoulos JA, Tsurutani AC, Zhu GD, Rosenberg SH, Giranda VL, Frost DJ (2007) ABT-888, an orally active poly(ADP-ribose) polymerase inhibitor that potentiates DNA-damaging agents in preclinical tumor models. Clin Cancer Res 13:2728–2737

13. Fukushima M, Kuzuya K, Ota K, Ikai K (1981) Poly(ADP-ribose) synthesis in human cervical cancer cell-diagnostic cytological usefulness. Cancer Lett 14:227–236
14. Graziani G, Szabo C (2005) Clinical perspectives of PARP inhibitors. Pharmacol Res 52:109–118
15. Hirai K, Ueda K, Hayaishi O (1983) Aberration of poly(adenosine diphosphate-ribose) metabolism in human colon adenomatous polyps and cancers. Cancer Res 43:3441–3446
16. Kummar S, Kinders R, Gutierrez M, Rubinstein L, Parchment RE, Phillips LR, Low J, Murgo AJ, Tomaszewski JE, Doroshow JH, Working Group NCI (2007) Inhibition of poly (ADP-ribose) polymerase (PARP) by ABT-888 in patients with advanced malignancies: results of a phase 0 trial. J Clin Oncol 25:3518a
17. Liu X, Palma J, Kinders R, Shi Y, Donawho C, Ellis PA, Rodriguez LE, Colon-Lopez M, Saltarelli M, LeBlond D, Lin CT, Frost DJ, Luo Y, Giranda VL (2008) An enzyme-linked immunosorbent poly(ADP-ribose) polymerase biomarker assay for clinical trials of PARP inhibitors. Anal Biochem 381:240–247
18. McCully CL, Balis FM, Bacher J, Phillips J, Poplack DG (1990) A rhesus monkey model for continuous infusion of drugs into cerebrospinal fluid. Lab Anim Sci 40:520–525
19. Miknyoczki SJ, Jones-Bolin S, Pritchard S, Hunter K, Zhao H, Wan W, Ator M, Bihovsky R, Hudkins R, Chatterjee S, Klein-Szanto A, Dionne C, Ruggeri B (2003) Chemopotentiation of temozolomide, irinotecan, and cisplatin activity by CEP-6800, a poly(ADP-ribose) polymerase inhibitor. Mol Cancer Ther 2: 371–382
20. Miwa M, Masutani M (2007) PolyADP-ribosylation and cancer. Cancer Sci 98:1528–1535
21. National Research Council (1996) Guide for the care and use of laboratory animals. National Academy Press, Washington
22. Perrier D, Mayersohn M (1982) Noncompartmental determination of the steady-state volume of distribution for any mode of administration. J Pharm Sci 71:372–373
23. Plummer ER (2006) Inhibition of poly(ADP-ribose) polymerase in cancer. Curr Opin Pharmacol 6:364–368
24. Ruscetti T, Lehnert BE, Halbrook J, Le Trong H, Hoekstra MF, Chen DJ, Peterson SR (1998) Stimulation of the DNA-dependent protein kinase by poly(ADP-ribose) polymerase. J Biol Chem 273:14461–14467
25. Satoh MS, Poirier GG, Lindahl T (1993) NAD(+)-dependent repair of damaged DNA by human cell extracts. J Biol Chem 268:5480–5487
26. Schreiber V, Ame JC, Dolle P, Schultz I, Rinaldi B, Fraulob V, Menissier-de Murcia J, de Murcia G (2002) Poly(ADP-ribose) polymerase-2 (PARP-2) is required for efficient base excision DNA repair in association with PARP-1 and XRCC1. J Biol Chem 277:23028–23036
27. Schreiber V, Dantzer F, Ame JC, de Murcia G (2006) Poly(ADP-ribose): novel functions for an old molecule. Nat Rev Mol Cell Biol 7:517–528
28. Shiobara M, Miyazaki M, Ito H, Togawa A, Nakajima N, Nomura F, Morinaga N, Noda M (2001) Enhanced polyadenosine diphosphate-ribosylation in cirrhotic liver and carcinoma tissues in patients with hepatocellular carcinoma. J Gastroenterol Hepatol 16:338–344
29. Tentori L, Graziani G (2005) Chemopotentiation by PARP inhibitors in cancer therapy. Pharmacol Res 52:25–33
30. Tentori L, Leonetti C, Scarsella M, D'Amati G, Vergati M, Portarena I, Xu W, Kalish V, Zupi G, Zhang J, Graziani G (2003) Systemic administration of GPI 15427, a novel poly(ADP-ribose) polymerase-1 inhibitor, increases the antitumor activity of temozolomide against intracranial melanoma, glioma, lymphoma. Clin Cancer Res 9:5370–5379
31. Tomoda T, Kurashige T, Moriki T, Yamamoto H, Fujimoto S, Taniguchi T (1991) Enhanced expression of poly(ADP-ribose) synthetase gene in malignant lymphoma. Am J Hematol 37:223–227
32. Wharton SB, McNelis U, Bell HS, Whittle IR (2000) Expression of poly(ADP-ribose) polymerase and distribution of poly(ADP-ribosyl)ation in glioblastoma and in a glioma multicellular tumour spheroid model. Neuropathol Appl Neurobiol 26:528–535
33. Wielckens K, Garbrecht M, Kittler M, Hilz H (1980) ADP-ribosylation of nuclear proteins in normal lymphocytes and in low-grade malignant non-Hodgkin lymphoma cells. Eur J Biochem 104:279–287